Physics Letters A 161 (1992) 499–505
North-Holland

PHYSICS LETTERS A

Chaotic dynamics due to competition among degenerate modes in a ring-cavity laser

Alejandro Aceves
Department of Mathematics and Statistics, University of New Mexico, Albuquerque, NM 87131, USA

Darryl D. Holm and Gregor Kovacic
Theoretical Division and Center for Nonlinear Studies, Los Alamos National Laboratory, MS B284, Los Alamos, NM 87545, USA

Received 25 September 1991; revised manuscript received 12 November 1991; accepted for publication 18 November 1991
Communicated by A.R. Bishop

Competition between two degenerate spatial modes in a ring-cavity laser is shown to lead to chaotic time evolution of their amplitudes. Analysis of this temporal chaos implies that the laser output will show randomly intermittent bursts of apparent spatial complexity due to interference between the two competing modes.

1. Introduction

The nonlinear dynamics of a ring–cavity laser is generally characterized by competition among modes that describe the spatial structure of the fields [1,2]. This competition appears experimentally in the measurement of time-dependent transverse spatial patterns in the laser intensity output [3]. In some cases, the ring–cavity resonator geometry can be adjusted, or tuned, to produce two degenerate modes, i.e. two modes with equal longitudinal wave numbers [1,2]. In the case of such a degeneracy, the dynamics of the mode competition simplifies to a system of ordinary differential equations for the time-dependent complex amplitudes of the two cavity modes (i.e., the transverse spatial structures of the fields). In this case, rigorous dynamical systems methods can be applied to exactly characterize the chaotic dynamics that results for the mode amplitudes. We show that this is a purely temporal type of chaos, although it manifests itself experimentally as chaotically changing transverse spatial patterns in the laser intensity output.

The geometry for a ring-cavity laser experiment with degenerate modes consists of a resonant cavity with curved end mirrors [1–3]. The ring-cavity laser dynamics is described by the Maxwell–Bloch equations for the slowly varying complex envelopes E and P of the electric field, $\mathscr{E}=\mathrm{Re}\{E\exp[\mathrm{i}(k_0z-\omega_0t)]\}$, the polarizability of the medium, $\mathscr{P}=\mathrm{Re}\{P\exp[\mathrm{i}(k_0z-\omega_0t)]\}$ and the real level inversion, D. Here k_0 and ω_0 are the wave number and frequency of the incident light. The Maxwell–Bloch equations are given by [1,2]

$$-\tfrac{1}{4}\mathrm{i}\nabla_\perp^2 E+\frac{\partial E}{\partial z}+\frac{\partial E}{\partial t}=P,\quad \frac{\partial P}{\partial t}=ED-\delta P,\quad \frac{\partial D}{\partial t}=-\mathrm{Re}(E^*P)-\delta(D-D_0)\,,$$

where $\nabla_\perp^2$ denotes the transverse Laplacian, longitudinal distance z is measured in units of Λ (the optical path length), time is measured in units of the round-trip time for light, Λ/c, and the small parameter $\delta=\gamma\Lambda/c\ll 1$ is the ratio of time scales: the round-trip time for light in the cavity, divided by the relaxation time of the medium. By choosing to scale time in units of Λ/c and setting $\delta=0$, we address dynamics on the nondissipative time scale, i.e., on a time scale which is short compared to any dissipation time.

We assume separation of variables for the solution of the linearly polarized electric field in the resonant cavity. Because these cavity modes are taken to be degenerate in longitudinal wave number, we may assume a solution in the form $E(r, \theta, z, t) = \sum_l A_l(r, \theta, z) E_l(t)$, where $A_l(r, \theta, z)$ describes the spatial structure of the lth empty-cavity field mode. That is, $A_l(r, \theta, z)$ is the lth eigenfunction in the cavity of the spatial part of the linear operator in the first Maxwell–Bloch equation (see, e.g., ref. [2], appendix A). Similar modal expansions are also assumed for the fields P and D. Substituting these three modal expansions into the Maxwell–Bloch equations and projecting onto the lth degenerate mode yields the following set of coupled Maxwell–Bloch (CMB) equations, labeled by indices l, m, $n = 1, ..., L$,

$$\dot{E}_l = P_l, \quad \dot{P}_l = \sum_{mn} \Gamma_{lmn} E_m D_n, \quad \dot{D}_l = -\mathrm{Re}\left(\sum_{mn} \Gamma_{lmn} E_m^* P_n\right). \tag{1}$$

In these CMB equations $\Gamma_{lmn} = \int_{\text{cavity}} A_l A_m A_n$. Consequently, the real arrays of constants Γ_{lmn} describing the coupling among the modes are totally symmetric tensors. That is, $\Gamma_{lmn} = \Gamma_{\sigma(lmn)}$ of every permutation σ of l, m, and n.

2. Diagonalization of the modal equations

The CMB equations (1) derived above possess L constants of motion, $K_l = \frac{1}{2}\sum_{mn} \Gamma_{lmn} E_m E_n^* + D_l$, $l = 1, ..., L$. The conserved quantity K_l is the projection onto the lth mode of the sum of the total field energy and atomic excitation energy, $\frac{1}{2}|E|^2 + D$. Since K_l is linear in D_l we may use it to eliminate D_l and thereby reduce the number of equations from $5L$ to $4L$. After this elimination, we have

$$\dot{E}_l = P_l, \quad \dot{P}_l = \sum_{mn}\left[\Gamma_{lmn} E_m \left(K_n - \tfrac{1}{2}\sum_{pq} \Gamma_{npq} E_p E_q^*\right)\right].$$

These equations describe a set of L coupled complex Duffing oscillators. They may be expressed in Hamiltonian form as $\dot{E}_l = \{E_l, H\} = 2\partial H/\partial P_l^*$ and $\dot{P}_l = \{P_l, H\} = 2\partial H/\partial E_l^*$, with Hamiltonian function

$$H = \sum_l \left[\tfrac{1}{2}|P_l|^2 + \tfrac{1}{2}\left(K_l - \tfrac{1}{2}\sum_{mn} \Gamma_{lmn} E_m E_n^*\right)^2\right]. \tag{2}$$

Now, $2H = \sum_l (|P_l|^2 + D_l^2)$, in terms of the original variables. Hence, conservation of H for the Duffing oscillator system represents preservation of the total unitarity of the system by the CMB dynamics (see ref. [4]). Invariance of the Hamiltonian H under the overall phase shift $(P_l, E_l) \to (e^{i\varphi} P_l, e^{i\varphi} E_l)$ also implies conservation of its infinitesimal generator, $J = \sum_l \mathrm{Im}(E_l^* P_l)$. This conserved quantity is the total self-interaction energy of the L modes.

Consider the situation in which the coupling coefficients Γ_{lmn} mutually commute, i.e., suppose

$$\sum_l (\Gamma_{lmn}\Gamma_{lpq} - \Gamma_{lmq}\Gamma_{lpn}) = 0 .$$

Then the total Hamiltonian, H in eq. (2), may be diagonalized. This diagonalization of H may be understood by regarding Γ_{lmn} as a set of L symmetric matrices, written $\Gamma_{mn}^{(l)}$. The commutation formula above means that the symmetric matrices $\Gamma^{(l)}$ and $\Gamma^{(j)}$ commute for all l and j. Hence, in this situation, a single orthogonal $L \times L$ matrix, O_{lm}, exists that simultaneously diagonalizes all the Γ matrices. Because of the total symmetry of the tensors Γ_{lmn}, which is preserved under orthogonal transformations, the only nonzero entry remaining in the jth tensor $\Gamma^{(j)}$ after such a diagonalization is $\Gamma_{jj}^{(j)} = \gamma_j$. Performing this orthogonal transformation on the fields E_l and P_l, and on the constants K_l, $(E_l, P_l, K_l) \to (E_l', P_l', K_l') = (\sum_m O_{lm} E_m, \sum_m O_{lm} P_m, \sum_m O_{lm} K_m)$, yields the Hamiltonian for the system in the new variables (after dropping the primes) in diagonalized form,

$$H=\sum_l H_l=\sum_l \left[\tfrac{1}{2}|P_l|^2+\tfrac{1}{2}(K_l-\tfrac{1}{2}\gamma_l|E_l|^2)^2\right].$$

Thus, the Hamiltonian decouples into a sum of L complex-Duffing-oscillator Hamiltonians, provided the coupling coefficients Γ_{lmn} mutually commute as symmetric matrices. In this case, the conserved Hamiltonians H_l of the decoupled modes are the projections of the unitarity condition for the full system onto each mode.

This diagonalization renders each Hamiltonian H_l invariant under an independent phase change of the lth fields: $(E_l, P_l)\to(\mathrm{e}^{\mathrm{i}\varphi_l}E_l, \mathrm{e}^{\mathrm{i}\varphi_l}P_l)$. Hence, the self-interaction energy for each mode, $J_l=\mathrm{Im}(E_l^*P_l)$, is separately conserved. These additional conservation laws imply that the dynamics of each decoupled Hamiltonian subsystem is completely integrable. Therefore, the entire system of L interacting ring-cavity modes is completely integrable when the coupling coefficients mutually commute.

3. The integrable decoupled model

The Hamiltonian and the conserved self-interaction energy for a single decoupled mode are given by

$$H_l=\tfrac{1}{2}|P_l|^2+\tfrac{1}{2}(K_l-\tfrac{1}{2}\gamma_l|E_l|^2)^2,\quad J_l=\mathrm{Im}(E_l^*P_l),$$

where conservation of J_l follows from phase invariance of H_l. This phase invariance suggests the canonical transformation to polar coordinates given by $E_l=\mathcal{Q}_l\,\mathrm{e}^{\mathrm{i}\varphi_l}$ and $P_l=(\mathcal{P}_l+\mathrm{i}J_l/\mathcal{Q}_l)\,\mathrm{e}^{\mathrm{i}\varphi_l}$. When expressed in these polar coordinates, the single-mode Hamiltonian is independent of φ_l,

$$H_l=\tfrac{1}{2}\mathcal{P}_l^2+J_l^2/2\mathcal{Q}_l^2+\tfrac{1}{2}(K_l-\tfrac{1}{2}\gamma_l\mathcal{Q}_l^2)^2,$$

and Hamilton's equations for $(\mathcal{Q}_l, \mathcal{P}_l, \varphi_l, J_l)$ are given by

$$\dot{\mathcal{Q}}_l=\{\mathcal{Q}_l, H_l\}=\mathcal{P}_l,\quad \dot{\mathcal{P}}_l=\{\mathcal{P}_l, H_l\}=\gamma_l\mathcal{Q}_l(K_l-\tfrac{1}{2}\gamma_l\mathcal{Q}_l^2)+J_l^2/\mathcal{Q}_l^3,\quad \dot{\varphi}_l=\{\varphi_l, H_l\}=J_l/\mathcal{Q}_l^2,\quad \dot{J}_l=\{J_l, H_l\}=0.$$

In the case $J_l=0$ and $K_l>0$, and only in this case, the solutions of this system have a homoclinic orbit in the $\mathcal{Q}_l$–$\mathcal{P}_l$ phase plane. In the original variables, the homoclinic solution of eqs. (1) for $J_l=0$ and $K_l>0$ is given by

$$E_l=2\sqrt{K_l/\gamma_l}\,\mathrm{sech}[\sqrt{K_l\gamma_l}\,(t-t_l)]\,\mathrm{e}^{\mathrm{i}\bar{\varphi}_l},\quad P_l=-2K_l\,\mathrm{sech}[\sqrt{K_l\gamma_l}\,(t-t_l)]\tanh[\sqrt{K_l\gamma_l}\,(t-t_l)]\,\mathrm{e}^{\mathrm{i}\bar{\varphi}_l}.$$

This solution connects the hyperbolic point at the origin, $E_l=0=P_l$, to itself. Geometrically the solution is a "pinched torus," i.e., the Cartesian product of a homoclinic loop in a plane $\varphi_l=\bar{\varphi}_l$ (which is constant for $J_l=0$), times a circle parameterized by the value of phase angle $\bar{\varphi}_l$. For $J_l\neq0$, all other solutions are periodic in the $\mathcal{Q}_l$–$\mathcal{P}_l$ phase plane and, thus, are quasiperiodic with two periods in the original variables. See ref. [4] for further details.

4. Recoupling the modes

In general, the coupling coefficients Γ_{lmn} do not mutually commute. Of particular interest is the situation in which they nearly commute, and are expressible as $\Gamma_{lmn}=\gamma_l\delta_{lmn}+\epsilon\Delta_{lmn}$, where $\delta_{lmn}=1$, if $l=m=n$, and vanishes otherwise. The coefficients Δ_{lmn} are assumed not to mutually commute with all the Γ_{lmn}, and ϵ is taken to be the small uniform coupling strength; $\epsilon\ll1$. We treat this situation as a nearly integrable problem, and ask what physical consequences arise when the coupling perturbation breaks integrability.

We consider the case of two coupled modes, $L=2$, which is the case most frequently encountered in experiments. Suppose the unperturbed modes before coupling have $J_1=0$, $K_1>0$, and $J_2\neq0$, so we are coupling a homoclinic structure in mode 1 with the quasiperiodic structure of mode 2, see fig. 1. Except for the ho-

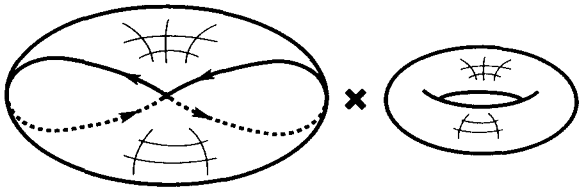

Fig. 1. The homoclinic CMB solutions in the two-mode phase space can be regarded geometrically as a pinched torus (mode 1) crossed into a two-torus (mode 2).

moclinic orbits, most solutions in this case are quasiperiodic with four (i.e., $2L$) frequencies. Thus, the pure second mode is a special solution, since it has only two frequencies. In the system of two modes, the solution corresponding to the pure second mode is hyperbolic; that is, it is unstable along the homoclinic orbits of the first mode. As a two-frequency quasiperiodic solution, the pure second mode can be thought of as a two-torus, and the unperturbed solutions homoclinic to it in the full phase space can be regarded geometrically as a pinched torus, crossed into the two-torus of the pure second mode, as shown in fig. 1. Therefore, the unperturbed orbits homoclinic to a particular pure second mode solution (for a particular choice of J_2 and K_2) form a four-dimensional homoclinic surface.

In the weakly coupled case, $\epsilon \neq 0$, most of the special solutions with just two frequencies still persist and are $O(\epsilon)$ close to the pure second-mode solutions. Moreover, the unstable directions of these perturbed solutions with only two frequencies are $O(\epsilon)$ close to the homoclinic directions of the unperturbed pure first-mode solution. (The validity of these claims follows from the persistence theory of normally hyperbolic manifolds and the KAM theorem, see, e.g., ref. [5].) Hence, orbits forward-asymptotic in time to any perturbed two-frequency quasiperiodic solution still form a smooth four-dimensional surface, which is $O(\epsilon)$ close to the unperturbed homoclinic surface. This surface is called the stable manifold of the perturbed two-frequency quasiperiodic solution. Likewise, orbits backward-asymptotic to a two-frequency quasiperiodic solution form its smooth four-dimensional unstable manifold.

If the two-mode system were to remain integrable under the weak coupling, then the stable and unstable manifolds of the hyperbolic quasiperiodic solution would continue to coincide, as a slightly deformed four-dimensional homoclinic surface. However, when, as expected, the coupling perturbation destroys integrability, the stable and unstable manifolds will, in general, intersect. These intersections are the homoclinic orbits of the hyperbolic solution that survive after the coupling. These homoclinic intersection orbits form two-dimensional surfaces, since they are the intersections of four-dimensional stable and unstable manifolds in the six-dimensional simultaneous level surfaces (lying in the eight-dimensional phase space) of the total unitarity H and self-interaction energy J.

5. Showing transverse intersections

In order to show that homoclinic intersections occur under weak coupling of the two modes, we use the standard Melnikov method [5,6]. Application of this method requires the computation of the distance between perturbed stable and unstable manifolds of the hyperbolic solutions, to first order in ϵ. This first-order distance is given by a vector having two components measured along two of the normal directions to the unperturbed homoclinic surface. For these directions we choose ∇H_1 and ∇J_1, the eight-component gradients in the full phase space of the conserved quantities for the unperturbed first mode. Only two normal directions (out of the existing four) are needed, because both the perturbed stable and unstable manifolds of the hyperbolic solution lie on level surfaces of total H and total J (see refs. [4,5]). These two components of the required first-order distance are given by

$$M_1 = \int_{-\infty}^{\infty} \nabla H \cdot \boldsymbol{g}\, \mathrm{d}t, \quad M_2 = \int_{-\infty}^{\infty} \nabla J_1 \cdot \boldsymbol{g}\, \mathrm{d}t\,,$$

where the integrals are taken along a particular unperturbed homoclinic orbit of mode 1, and the eight-component vector $\boldsymbol{g}$ is the linearization in ϵ of the perturbed flow. In terms of the field, we have

$$M_1 = \int_{-\infty}^{\infty} \mathrm{d}t \sum_{mn} \Delta_{1mn}[(K_m - \tfrac{1}{2}\gamma_m |E_m|^2)\,\mathrm{Re}(E_n^* P_1) - \tfrac{1}{2}\gamma_1\, \mathrm{Re}(E_m E_n^* E_1^* P_1)]\,,$$

$$M_2 = \int_{-\infty}^{\infty} \mathrm{d}t \sum_{mn} \Delta_{1mn}(K_m - \tfrac{1}{2}\gamma_m |E_m|^2)\,\mathrm{Im}(E_1^* E_n)\,,$$

where E_m is evaluated at $t - t_m$ and φ_m along the unperturbed homoclinic and quasiperiodic solutions.

In order to compute the Melnikov vector components (M_1, M_2), we begin by considering the unperturbed motion in the $(\mathcal{Q}_2, \mathcal{P}_2)$ phase plane of the second mode and linearizing this motion in the vicinity of the center at $\mathcal{Q}_2 = \bar{Q}_2$ and $\mathcal{P}_2 = 0$. This linearized solution undergoes *harmonic* motion in the $(\mathcal{Q}_2, \mathcal{P}_2)$ phase plane. In the full phase space, these harmonic motions are given in terms of the complex envelope field variables (E_2, P_2) by

$$E_2 = \{\bar{Q}_2 + A_2 \cos[\Omega(t-t_2)] - (2\mathrm{i}\omega A_2/\Omega)\sin[\Omega(t-t_2)]\}\exp[\mathrm{i}\omega(t-t_2) + \mathrm{i}\bar{\varphi}_2]\,,$$

$$P_2 = \{\mathrm{i}\bar{Q}_2\omega + (A_2/\Omega)(2\omega^2 - \Omega^2)\sin[\Omega(t-t_2)] - \mathrm{i}A_2\omega\cos[\Omega(t-t_2)]\}\exp[\mathrm{i}\omega(t-t_2) + \mathrm{i}\bar{\varphi}_2]\,,$$

where we denote $\omega = J_2/\bar{Q}_2^2$, $\Omega^2 = \gamma_2^2 \bar{Q}_2^2 + 4\omega^2$, and t_2 and $\bar{\varphi}_2$ are constant parameters.

Substituting into the integrands of the Melnikov vector the expressions for the unperturbed homoclinic mode-1 solution (E_1, P_1) given earlier and the linearized quasiperiodic mode-2 solution (E_2, P_2) given above yields, after considerable algebra and evaluation of integrals,

$$M_1 = a_1 \sin(\omega\,\Delta t - \Delta\bar{\varphi}) + a_2 \sin[(\Omega+\omega)\,\Delta t - \Delta\bar{\varphi}] + a_3 \sin[(\Omega-\omega)\,\Delta t - \Delta\bar{\varphi}] + a_4 \sin(\Omega\,\Delta t)\,,$$

$$M_2 = b_1 \sin(\omega\,\Delta t - \Delta\bar{\varphi}) + b_2 \sin[(\Omega+\omega)\,\Delta t - \Delta\bar{\varphi}] + b_3 \sin[(\Omega-\omega)\,\Delta t - \Delta\bar{\varphi}]\,,$$

where $\Delta t = t_1 - t_2$, $\Delta\bar{\varphi} = \bar{\varphi}_1 - \bar{\varphi}_2$, and the coefficients a_i and b_j are given below,

$$a_1 = \frac{\pi}{\gamma_1}\bar{Q}_2\omega\,\mathrm{sech}\left(\frac{\pi\omega}{2\sqrt{K_1\gamma_1}}\right)\left[\tfrac{2}{3}K_1\left(1 + \frac{K_1}{K_2}\Delta_{112} - \frac{3\omega^2}{K_1\gamma_1}\right) - \gamma_2\bar{Q}_2^2\Delta_{122}\right],$$

$$a_2 = \frac{\pi A_2\omega}{\gamma_1}\left(1 - \frac{\Omega}{\omega}\right)\mathrm{sech}\left(\frac{\pi(\omega-\Omega)}{2\sqrt{K_1\gamma_1}}\right)\left[\tfrac{2}{3}K_1\left(\frac{1}{2} + \frac{\omega}{\Omega}\right)\left(1 + \frac{K_1}{K_2} - \frac{3(\omega-\Omega)^2}{K_1\gamma_1}\right)\Delta_{112} - \gamma_2\left(\frac{3}{2} + \frac{\omega}{\Omega}\right)\Delta_{122}\right],$$

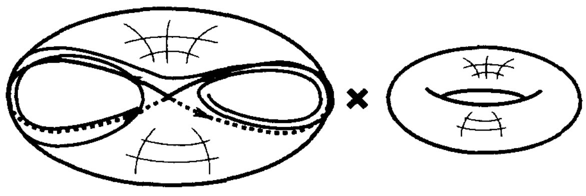

Fig. 2. The weak-coupling perturbation causes transverse intersections of the stable and unstable manifolds of the homoclinic solutions to occur near $\Delta t = 0$ and $\Delta\bar{\varphi} = 0$, or π. A typical orbit near these transverse intersections switches randomly from side to side in the vicinity of the homoclinic periodic orbit and near the plane containing $\Delta\bar{\varphi} = 0$ and $\Delta\bar{\varphi} = \pi$.

$$a_3=\frac{\pi A_2\omega}{\gamma_1}\left(1+\frac{\Omega}{\omega}\right)\operatorname{sech}\left(\frac{\pi(\omega+\Omega)}{2\sqrt{K_1\gamma_1}}\right)\left[\tfrac{2}{3}K_1\left(\frac{1}{2}-\frac{\omega}{\Omega}\right)\left(1+\frac{K_1}{K_2}-\frac{3(\omega+\Omega)^2}{K_1\gamma_1}\right)\Delta_{112}-\gamma_2\left(\frac{3}{2}-\frac{\omega}{\Omega}\right)\Delta_{122}\right],$$

$$a_4=-\frac{2\pi A_2}{\gamma_1}\left(\Delta_{122}+\frac{\gamma_1}{\gamma_2}\Delta_{112}\right)\frac{\bar{Q}_2\Omega^2}{\sinh^2(\pi\Omega/2\sqrt{K_1\gamma_1})},$$

$$b_1=-\frac{2\pi\bar{Q}_2}{\gamma_1}\operatorname{sech}\left(\frac{\pi\omega}{2\sqrt{K_1\gamma_1}}\right)\left[\Delta_{112}\left(2K_1+\frac{\omega^2}{\gamma_1}\right)+\Delta_{122}\left(K_2-\frac{\gamma_2}{2\bar{Q}_2^2}\right)\right],$$

$$b_2=-\frac{2\pi A_2}{\gamma_1}\operatorname{sech}\left(\frac{\pi(\omega-\Omega)}{2\sqrt{K_1\gamma_1}}\right)\left(\frac{1}{2}+\frac{\omega}{\Omega}\right)\left[\Delta_{112}\left(2K_1+\frac{(\omega-\Omega)^2}{\gamma_1}\right)+\Delta_{122}(K_2-\gamma_2\bar{Q}_2^2)\right],$$

$$b_3=-\frac{2\pi A_2}{\gamma_1}\operatorname{sech}\left(\frac{\pi(\omega+\Omega)}{2\sqrt{K_1\gamma_1}}\right)\left(\frac{1}{2}-\frac{\omega}{\Omega}\right)\left[\Delta_{112}\left(2K_1+\frac{(\omega+\Omega)^2}{\gamma_1}\right)+\Delta_{122}(K_2-\gamma_2\bar{Q}_2^2)\right].$$

The Melnikov vector components M_1 and M_2 have simultaneous zeros, when $\Delta t=0$ and $\Delta\bar{\varphi}=0$, or π. (Since the Jacobian $(\partial M_1, \partial M_2)/(\partial\Delta t, \Delta\bar{\varphi})$ is nonvanishing, these Melnikov zeros are simple.) Hence, the consequence of coupling small-amplitude oscillations of mode 2 to mode 1 is to produce transverse intersections of the stable and unstable manifolds of the hyperbolic quasiperiodic solutions of the coupled system. These transverse intersections are sketched in fig. 2. The formulas for M_1 and M_2 show that the transverse intersections caused by mode coupling are two-dimensional and parameterized either by $t-t_2$ and $\bar{\varphi}_2$, or, equivalently, by $t-t_1$ and $\bar{\varphi}_1$. As shown in the next section, these transverse intersections imply chaotic dynamics for phase points in their vicinity via a Smale horseshoe construction.

6. Generalized Smale horseshoe construction

We consider the Poincaré map Φ obtained by taking a Poincaré section at $t-t_2=0$, modulo 2π. In the φ_2-reduced phase space $(\mathcal{Q}_2, \mathcal{P}_2)$ for the linearized harmonic mode-2 motion, this Poincaré section is the positive $\mathcal{Q}_2$ axis. In the Poincaré section the quasiperiodic mode-2 solution is a circle, and the Poincaré map Φ takes this circle into itself. This circle is hyperbolic in the phase space for the coupled system and, according to the Melnikov calculation just given, its stable and unstable manifolds intersect transversely. These transverse intersections are two-dimensional surfaces in the continuous-time dynamics, and in our Poincaré section they are circles (rather than points, as in the usual Poincaré section). The angle parameterizing each intersection circle in the Poincaré section is $\bar{\varphi}_2$, or, equivalently, φ, the angle conjugate to the total interaction energy, J_{tot}. Because J_{tot} is conserved, the dynamics for φ decouples from the rest of the system and may now be factored out by Hamiltonian reduction. The transverse intersections on the resulting *reduced* Poincaré section form the usual homoclinic tangle of points, as guaranteed by the Poincaré–Birkhoff–Smale theorem. That is, an iterate of the reduced Poincaré map results in a Smale horseshoe construction, thereby leading to an invariant Cantor set of points in the reduced Poincaré section on which the dynamics is topologically conjugate to a Bernoulli shift [5,6]. Adding back the angle φ now yields an invariant Cantor set of *circles*, whose dynamics under the reconstructed Poincaré map is extremely sensitive to initial conditions.

7. Physical implications

Given that the dynamics in the vicinity of the homoclinic tangle is chaotic, what implications are there for ring-cavity laser experiments? For phase points in the vicinity of the homoclinic tangle, the time series for the amplitude of the first mode $|E_1|$ will show intermittent excursions away from zero in the form of the homoclinic solution,

$$|E_1| = 2\sqrt{K_1/\gamma_1}\ \mathrm{sech}[\sqrt{K_1\gamma_1}\ (t-t_\mu)]\ ,$$

where t_μ is now indistinguishable from a *random* variable, because of the extreme sensitivity to initial conditions for this motion. These intermittent bursts in the first mode will interfere with the quasiperiodic evolution of the second mode, in the total output intensity of the laser,

$$|E|^2 = |E_1(t)\,A_1(r,\theta,z) + E_2(t)\,A_2(r,\theta,z)|^2\ ,$$

where $A_1(r, \theta, z)$ and $A_2(r, \theta, z)$ represent the two transverse spatial patterns of the competing degenerate cavity modes. Hence the resulting transverse spatial pattern of the total resulting laser output will show a chaotic sequence of bursts of interference. During these bursts, the transverse output will appear spatially complex. Thus an effect which might appear to be spatio-temporal chaos is actually due to temporal chaos alone, arising from the competition between two degenerate spatial modes.

Acknowledgement

This work was partially supported by the US Air Force Office of Scientific Research, contract numbers AFOSR-91-0009 and AFOSRISSA900024. The authors would like to thank Roberto Camassa, Tasso Kaper, and Vittorio Penna for their constructive comments and encouragement.

References

[1] L.A. Lugiato, G.L. Oppo, J.R. Tredicce, L.M. Narducci and M.A. Pernigo, J. Opt. Soc. Am. B 7 (1990) 1019;
M. Brambila, F. Battipede, L.A. Lugiato, V. Penna, F. Prati, C. Tamm and C.O. Weiss, Phys. Rev. A 43 (1991) 5090.
[2] C. Tamm and C.O. Weiss, J. Opt. Soc. Am. B 7 (1990) 1034.
[3] G. Giusfredi, J.F. Valley, R. Pon, G. Khitrova and H.M. Gibbs, J. Opt. Soc. Am. B 5 (1988) 1181.
[4] D.D. Holm, G. Kovacic and B. Sundaram, Phys. Lett. A 154 (1991) 346.
[5] S. Wiggins, Global bifurcations and chaos: analytical methods (Springer, Berlin, 1988).
[6] J. Guckenheimer and P.J. Holmes, Nonlinear oscillations, dynamical systems, and bifurcations of vector fields (Springer, Berlin, 1983).